Genetic loss of *Tmprss6* alters terminal erythroid differentiation in a mouse model of β-thalassemia intermedia

David B. Stagg,[1] Rebecca L. Whittlesey,[2*] Xiuqi Li,[3*] Larisa Lozovatsky,[3] Sara Gardenghi,[4,5] Stefano Rivella[4,5,6] and Karin E. Finberg[1,3]*

[*]RLW and XL contributed equally to this work.

[1]Department of Pathology, Duke University School of Medicine, Durham, North Carolina, USA; [2]Department of Pharmacology and Cancer Biology, Duke University School of Medicine, Durham, North Carolina, USA; [3]Department of Pathology, Yale School of Medicine, New Haven, Connecticut, USA; [4]Department of Pediatrics, Division of Hematology-Oncology, Weill Cornell Medical College, New York, NY, USA; [5]Department of Cell and Developmental Biology, Weill Cornell Medical College, New York, NY, USA and [6]Department of Pediatrics, Children's Hospital of Philadelphia, Philadelphia, PA, USA

Correspondence: KARIN E. FINBERG - karin.finberg@yale.edu
doi:10.3324/haematol.2018.213371

SUPPLEMENTARY DATA

Genetic loss of *Tmprss6* alters terminal erythroid differentiation in a mouse model of β-thalassemia intermedia

David B. Stagg, Rebecca L. Whittlesey, Xiuqi Li, Larisa Lozovatsky, Sara Gardenghi, Stefano Rivella, and Karin E. Finberg

Supplementary Methods

Animal strains

Tmprss6$^{-/-}$ mice (B6.129P2-*Tmprss6*^{tm1Dgen}/Crl)(1) from Deltagen were backcrossed to C57BL/6N mice for ≥7 generations prior to study. *Hbb*$^{th3/+}$ mice on a C57BL/6J background (B6.129P2-*Hbb-b1*^{tm1Unc}*Hbb-b2*^{tm1Unc}/J)(2) were provided by one of the authors (S.R.). Experimental mice were bred and housed in the Duke University barrier facility under Institutional Animal Care & Use Committee approval, with food and water provided *ad libitum*. *Tmprss6*$^{+/-}$ mice were bred to *Hbb*$^{th3/+}$ mice to generate *Hbb*$^{th3/+}$*Tmprss6*$^{+/-}$ males, which were bred to *Tmprss6*$^{+/-}$ females to produce littermates of different *Hbb-Tmprss6* genotypes for phenotypic study. Mice were genotyped by polymerase chain reaction (PCR) using genomic DNA prepared from toe clips as template and using primers recognizing the targeted *Hbb* locus (forward 5'-GGCAAAGGATGTGATACGTGGAAG-3', reverse 5'- CCAGTTTCACTAATGACACAAACATG-3') and previously described primers recognizing the wild-type and mutant *Tmprss6* alleles.(1) Mice were fed either PicoLab Mouse Diet 20 [200 parts per million (p.p.m.). iron)] or 5T40 Modified Laboratory Rodent Diet 5001 (270 p.p.m. iron with 150 p.p.m. fenbendazole for pinworm prophylaxis) (both PMI Nutrition International). Pinworm prophylaxis was required because of an infection elsewhere in the animal facility; the mice in this study were not infected. Within a given *Hbb-Tmprss6* genotype, hemoglobin and hematocrit on either diet were similar, while subtle differences in red cell indices were observed (*Supplementary Table 3*). Within a given experiment, only sex, age, and diet-matched mice were studied, as indicated in each figure or table legend.

Hematologic and iron parameters in blood and tissues

Venous blood was collected from the retroorbital plexus under Avertin anesthesia. Complete blood counts were performed on a CellDyn 3700 (Abbott), using whole blood collected with heparinized capillary tubes into EDTA-coated Microvette tubes (Sarstedt). Peripheral blood smears were prepared by the Duke University Veterinary Diagnostics Laboratory. Blood smears were stained by a modified Wright-Giemsa method (JorVet Dip-Quick, Jorgensen Laboratories). Manual reticulocyte counts were performed on peripheral smears stained with new methylene blue (Jorgensen Laboratories) by examination of at least 1000 red cells. Brightfield images were acquired using the 100X/1.30 NA objective lens of an Eclipse E600 microscope (Nikon) with attached Spot RT Digital Camera and Spot 4.5 software (Diagnostic Instruments). The entire image was adjusted for brightness and contrast to match the original slide and labeled using Adobe Photoshop CS3 software with no further modifications. Using serum prepared in serum separator tubes (Beckton, Dickinson), serum iron concentration and total iron binding capacity were determined by the ferene method (Iron/UIBC kit, Thermo Scientific). Transferrin saturation was calculated as serum iron ÷ total iron binding capacity. Serum erythropoietin was determined by Quantikine Mouse/Rat Immunoassay (R&D Systems). Tissue non-heme iron concentrations were measured by the bathophenathroline method.(3)

Histological analysis of spleen

Mouse spleens were fixed in 10% buffered formalin for 24 hours. Following transfer to 70% ethanol, spleens were embedded in paraffin, and 8-micrometer sections were prepared by Duke University Medical Center Research Histology Laboratory. Deparaffinized tissue sections were stained with hematoxylin and eosin. Brightfield images were acquired at room temperature in the Yale Liver Center on an Olympus BX51 microscope with attached DP72 digital camera using cellSens software. The whole image was adjusted for brightness and contrast to match the original slide and labeled using Adobe Photoshop CS3 with no further modifications.

RNA extraction and quantitative reverse-transcription PCR

Following exsanguination under Avertin anesthesia, successful euthanasia was confirmed by collection of vital murine organs, which were flash-frozen in liquid nitrogen and stored at -80°C. RNA was subsequently prepared from homogenized liver and spleen using Trizol (Invitrogen) with DNase I treatment (Invitrogen). Bone marrow cells were flushed from mouse femur with RNase-free 1X phosphate-buffered saline (PBS) using a 25-gauge needle. Following passage through a 70μm cell strainer, the bone marrow cells were washed in PBS, homogenized using a QIAshredder (Qiagen), and stored at -80°C prior to total RNA isolation using the RNeasy Mini Kit with on-column DNase digestion (Qiagen). RNA from each tissue (0.5 μg) was reverse transcribed using the iScript cDNA Synthesis Kit (Bio-Rad). Transcript abundance was quantified by 2-step PCR (5 minutes at 95°C, followed by 45 cycles of 10 seconds at 95°C and 45 seconds at 60°C) in duplicate reactions using either iScript SYBR Green Supermix (Bio-Rad) on an iQ5 Multicolor Real-Time PCR Detection System (Bio-Rad) at Duke University Medical Center or iTaq Universal SYBR Green Supermix (Bio-Rad) on an ABI7500 Real-Time PCR System at the Yale School of Medicine. Primers pairs are described in *Supplementary Table 4*.

Analysis of membrane-bound globins

Whole blood was collected from the retroorbital plexus under Avertin anesthesia using heparinized capillary tubes. After one wash in 1X PBS, 1.5 $x10^8$ erythrocytes, as calculated from the RBC value of the complete blood count, were lysed in 0.05X PBS containing 1% protease inhibitors (Sigma, P8340) for 10 minutes on ice. After centrifugation at 13800g for 30 minutes, the pellet was cleared by 5 washes in 0.05X PBS. A final, more stringent wash in 0.02X PBS was then performed to maximize hypotonic lysis and thus minimize sample contamination by cytosolic globin chains. Membrane lipids were extracted by incubation in 56mM sodium borate (pH 8.0)

containing 1% protease inhibitors and 0.1% Tween-20. Following centrifugation at 13800g for 30 minutes, the pellet was flash-frozen and stored at -80°C. The pellet was subsequently dissolved in 8M urea, 10% acetic acid, 10% β-mercaptoethanol, and 0.04% pyronin. Globins were fractionated by triton-acetic acid-urea gel electrophoresis(4) and visualized by Coomassie stain. The stained gel was photographed using an Epson Perfection V750 Pro Scanner and acquired using Photoshop CS4 Version 11.0.

Flow cytometry

Bone marrow and spleen were harvested following mouse exsanguination under Avertin anesthesia. Bone marrow cells were flushed from mouse femur with 1X PBS/0.5% bovine serum albumin (BSA) using a 25-gauge needle. Spleens were mechanically disrupted in 1X PBS/0.5% BSA. Following passage through a 70-μm cell strainer, the bone marrow and spleen cells were pelleted and resuspended in 1X PBS/0.5% BSA. For each sample, 1.5 $x10^6$ cells were incubated with 0.5μg rat anti-mouse CD16/CD32 (BD Biosciences no. 553142) for 10 minutes on ice. Samples were then co-incubated for 30 minutes on ice in the dark with 1μg of the following rat anti-mouse antibodies: APC TER-119 (BD Biosciences, no. 557909), PE CD44 (BD Biosciences, no. 553134), and (for a subset) FITC CD71 (BD Biosciences, no. 553266). Triple-stained cells were washed twice and resuspended in 1X PBS/0.5% BSA prior to analysis. Cells doubly-stained with TER-119 and CD44 were washed and resuspended in PBS, and an aliquot of this cell suspension was analyzed for apoptosis using the FITC Annexin V kit (BD Biosciences) according to the manufacturer's instructions. The remainder of the cell suspension was treated with the ROS indicator CM-H_2DCFDA (Invitrogen) at a final concentration of 10μM for 15 minutes in the dark at 37°C in 5% CO_2, and cells were washed and resuspended in PBS prior to analysis. Fluorescence was quantified within one hour by the Duke University Flow Cytometry Shared Resource on a FACSCalibur (BD Biosciences). Flow cytometry data were analyzed using FlowJo software (Tree

Star). Stages of erythroid maturation were determined using forward scatter and expression levels of TER-119 and CD44,(5) and within each erythroid subpopulation, CD71 expression, apoptosis, and ROS were determined.(6) Representative plots are shown in *Supplementary Figure 9*.

Statistical analyses

Two-way repeated-measures ANOVA was performed using GraphPad Prism 7 to compare the distribution of EP among regions I, II, III, and IV in mice of different genotypes. All other comparisons were performed by unpaired, 2-tailed Student's t tests using Microsoft Excel for Mac software. *P* values less than .05 were considered statistically significant.

Supplementary Table 1. Physical, hematological, and serum parameters of 8-week-old female mice of all *Hbb*-*Tmprss6* genotype combinations fed a 270 p.p.m. iron diet.

		Whole Blood								Serum	
Genotype	Body wt, g	RBC, X 10^{12}/L	Hgb, g/L	Hct	MCV, X 10^{-15}L	MCH, pg	MCHC, g/L	RDW, %	Retic, %	Iron, μM	TS, %
$Hbb^{+/+}Tmprss6^{+/+}$	19 ± 1	9.2 ± 0.2	150 ± 5	0.457 ± 0.012	49.5 ± 0.6	16.2 ± 0.5	328 ± 8	17.7 ± 0.9	0.7 ± 0.1	28 ± 5	66 ± 7
$Hbb^{+/+}Tmprss6^{+/-}$	18 ± 1	9.2 ± 0.2	149 ± 4	0.449 ± 0.010	48.6 ± 0.5*	16.1 ± 0.4	331 ± 7	17.7 ± 0.7	0.5 ± 0.1	25 ± 2	59 ± 5
$Hbb^{+/+}Tmprss6^{-/-}$	18 ± 3	11.7 ± 0.7†	103 ± 10†	0.321 ± 0.019†	27.5 ± 0.9†	8.8 ± 0.5†	319 ± 12	42.4 ± 5.1†	7.0 ± 2.7*	10 ± 1†	26 ± 7†
$Hbb^{th3/+}Tmprss6^{+/+}$	18 ± 2	7.1 ± 0.4†‡	94 ± 4†§	0.304 ± 0.015†	42.6 ± 0.9†‡	13.1 ± 0.2†‡	308 ± 3†§	47.7 ± 2.7†§	33.7 ± 4.1*§	26 ± 3‡	56 ± 8*‡
$Hbb^{th3/+}Tmprss6^{+/-}$	17 ± 1†	7.5 ± 0.4†‡	94 ± 2†§	0.306 ± 0.012†	40.9 ± 1.1†‡‖	12.6 ± 0.5†‡¶	309 ± 6†§	46.7 ± 3.7†	23.7 ± 2.9*§¶	25 ± 6‡	56 ± 10*‡
$Hbb^{th3/+}Tmprss6^{-/-}$	17 ± 1	11.2 ± 0.2†‖	94 ± 3†§	0.306 ± 0.007†§	27.3 ± 0.8†‖	8.4 ± 0.3†‖	307 ± 4†§	39.2 ± 2.3†‖	5.8 ± 2.3*|	10 ± 2†‖	22 ± 3†‖

Body weight (wt), complete blood count, reticulocyte count (Retic), serum iron, and transferrin saturation (TS) were measured in 8-week-old female mice. Data are presented as means ± SD. RBC indicates red cell count; Hgb, hemoglobin; Hct, hematocrit; MCV, mean corpuscular volume; MCH, mean corpuscular hemoglobin; MCHC, mean corpuscular hemoglobin concentration; and RDW, red cell distribution width. *P<.05 compared with $Hbb^{+/+}Tmprss6^{+/+}$; †P<.005 compared with $Hbb^{+/+}Tmprss6^{+/+}$; ‡P<.005 compared with $Hbb^{+/+}Tmprss6^{-/-}$; §P<.05 compared with $Hbb^{+/+}Tmprss6^{-/-}$; ||P<.005 compared with $Hbb^{th3/+}Tmprss6^{+/+}$; and ¶P<.05 compared with $Hbb^{th3/+}Tmprss6^{+/+}$ mice. For wt, complete blood count, and SI, the number of mice per genotype analyzed was as follows, with exceptions shown in parentheses: 7 $Hbb^{+/+}Tmprss6^{+/+}$ (6 for SI/TS), 8 $Hbb^{+/+}Tmprss6^{+/-}$, 9 $Hbb^{+/+}Tmprss6^{-/-}$ (8 for SI/TS), 7 $Hbb^{th3/+}Tmprss6^{+/+}$, 9 $Hbb^{th3/+}Tmprss6^{+/-}$, and 6 $Hbb^{th3/+}Tmprss6^{-/-}$ (7 for wt and SI/TS). Reticulocytes were counted in 3-5 mice per genotype.

Supplementary Table 2. Physical and hematological parameters of 8-week-old male mice of all *Hbb-Tmprss6* genotype combinations fed a 270 p.p.m. iron diet.

		Whole Blood						
Genotype	Body wt, g	RBC, X 10^{12}/L	Hgb, g/L	Hct	MCV, X 10^{-15}L	MCH, pg	MCHC, g/L	RDW, %
Hbb$^{+/+}$*Tmprss6*$^{+/+}$	22 ± 2	9.2 ± 0.2	148 ± 3	0.457 ± 0.009	49.5 ± 0.5	16.0 ± 0.3	324 ± 4	17.6 ± 0.7
Hbb$^{+/+}$*Tmprss6*$^{+/-}$	23 ± 2	9.5 ± 0.3	147 ± 4	0.453 ± 0.018	47.9 ± 0.8*	15.6 ± 0.3*	325 ± 7	18.2 ± 0.7
Hbb$^{+/+}$*Tmprss6*$^{-/-}$	20 ± 2†	11.3 ± 0.8*	96 ± 8*	0.307 ± 0.017*	27.2 ± 0.8*	8.5 ± 0.2*	313 ± 8†	39.6 ± 2.7*
Hbb$^{th3/+}$*Tmprss6*$^{+/+}$	23 ± 2‡	7.4 ± 0.4*‡	94 ± 5*	0.303 ± 0.014*	40.9 ± 0.8*‡	12.7 ± 0.3*‡	310 ± 5*	45.4 ± 4.0*‡
Hbb$^{th3/+}$*Tmprss6*$^{+/-}$	23 ± 2‡	7.7 ± 0.3*‡	93 ± 3*	0.303 ± 0.010*	39.4 ± 1.8*‡	12.1 ± 0.5*‡‖	308 ± 4*	43.7 ± 4.7*
Hbb$^{th3/+}$*Tmprss6*$^{-/-}$	20 ± 2†§	11.0 ± 0.6*§	89 ± 5*‖¶	0.289 ± 0.014*‖¶	26.3 ± 0.7*§¶	8.1 ± 0.2*§‡	307 ± 5*	38.8 ± 2.8*§

Body wt and complete blood count were measured in 8-week-old male mice. *P<.005 compared with *Hbb*$^{+/+}$*Tmprss6*$^{+/+}$; †P<.05 compared with *Hbb*$^{+/+}$*Tmprss6*$^{+/+}$; ‡P<.005 compared with *Hbb*$^{+/+}$*Tmprss6*$^{-/-}$; §P<.005 compared with *Hbb*$^{th3/+}$*Tmprss6*$^{+/+}$; ‖P<.05 compared with *Hbb*$^{th3/+}$*Tmprss6*$^{+/+}$; and ¶P<.05 compared with *Hbb*$^{+/+}$*Tmprss6*$^{-/-}$ mice. For each parameter shown, the number of mice per genotype analyzed was as follows: 7 *Hbb*$^{+/+}$*Tmprss6*$^{+/+}$, 13 *Hbb*$^{+/+}$*Tmprss6*$^{+/-}$, 8 *Hbb*$^{+/+}$*Tmprss6*$^{-/-}$, 11 *Hbb*$^{th3/+}$*Tmprss6*$^{+/+}$, 8 *Hbb*$^{th3/+}$*Tmprss6*$^{+/-}$, and 9 *Hbb*$^{th3/+}$*Tmprss6*$^{-/-}$. Data are presented as means ± SD. Abbreviations are defined in *Supplementary Table 1*.

Supplementary Table 3. Hematological parameters of 8-week-old male mice of all *Hbb-Tmprss6* genotype combinations fed a 200 p.p.m. iron diet.

	Whole Blood						
Genotype	RBC, X 10^{12}/L	Hgb, g/L	Hct	MCV, X 10^{-15}L	MCH, pg	MCHC, g/L	RDW, %
Hbb$^{+/+}$*Tmprss6*$^{+/+}$	9.3 ± 0.4	144 ± 5	0.438 ± 0.016	46.9 ± 0.3*	15.5 ± 0.1*	329 ± 3†	17.6 ± 0.6
Hbb$^{+/+}$*Tmprss6*$^{+/-}$	9.3 ± 0.7	140 ± 10	0.425 ± 0.033	45.5 ± 0.6*	15.0 ± 0.4*	330 ± 5	18.1 ± 2.1
Hbb$^{+/+}$*Tmprss6*$^{-/-}$	11.9 ± 0.4	98 ± 5	0.302 ± 0.011	25.3 ± 0.6*	8.3 ± 0.3	326 ± 8†	39.1 ± 2.2
Hbb$^{th3/+}$*Tmprss6*$^{+/+}$	7.8 ± 0.6	91 ± 6	0.301 ± 0.010	38.7 ± 2.0	11.7 ± 0.2*	302 ± 13	46.1 ± 3.3
Hbb$^{th3/+}$*Tmprss6*$^{+/-}$	8.2 ± 0.3†	91 ± 4	0.290 ± 0.011	35.4 ± 0.8*	11.2 ± 0.2*	316 ± 5†	39.1 ± 1.6*
Hbb$^{th3/+}$*Tmprss6*$^{-/-}$	11.5 ± 0.6	90 ± 7	0.290 ± 0.014	25.3 ± 0.8	7.8 ± 0.3	309 ± 19	36.9 ± 1.3

Complete blood count were measured in male mice (8-9 weeks old) fed a 200 p.p.m. diet. *Significantly lower (*P*<.05) than the corresponding parameter in sex-and-genotyped-matched mice fed a 270 p.p.m. iron diet shown in *Supplementary Table 2.* †Significantly higher (*P*<.05) than corresponding parameter in sex-and-genotyped-matched mice fed a 270 p.p.m. iron diet shown in *Supplementary Table 3.* For each parameter shown, the number of mice per genotype analyzed was as follows: 4 *Hbb*$^{+/+}$*Tmprss6*$^{+/+}$, 5 *Hbb*$^{+/+}$*Tmprss6*$^{+/-}$, 5 *Hbb*$^{+/+}$*Tmprss6*$^{-/-}$, 4 *Hbb*$^{th3/+}$*Tmprss6*$^{+/+}$, 4 *Hbb*$^{th3/+}$*Tmprss6*$^{+/-}$, and 4 *Hbb*$^{th3/+}$*Tmprss6*$^{-/-}$. Data are presented as means ± SD. Abbreviations are defined in *Supplementary Table 1*.

Supplementary Table 4. Primer pairs used for quantitative RT-PCR analyses.

Gene	Forward Primer (5'-to-3')	Reverse Primer (5'-to-3')	Reference
Actb	ACCCACACTGTGCCCATCTA	CACGCTCGGTCAGGATCTTC	(7)
Ahsp	AGGACCTTTCTGAAGTCCAAAGAG	TGATGCCCAGACCCTTTAAGTT	(8)
Atoh8	CACCATCAGCGCAGCCTTC	CCATAGGAGTAGCACGGCACC	(9)
Bmp2	GACTGCGGTCTCCTAAAGGTCG	CTGGGGAAGCAGCAACACTA	(10)
Bmp6	ATGGCAGGACTGGATCATTGC	CCATCACAGTAGTTGGCAGCG	(9)
Erfe	ATGGGGCTGGAGAACAGC	TGGCATTGTCCAAGAAGACA	(11)
Epo	AGGAGGCAGAAAATGTCACG	CCACCTCCATTCTTTTCCAA	(12)
Gdf15	AGCCGAGAGGACTCGAACTCAG	GGTTGACGCGGAGTAGCAGCT	(13)
Hamp	CTGAGCAGCACCACCTATCTC	TGGCTCTAGGCTATGTTTTGC	(7)
*Hba**	GAAGCCCTGGAAAGGATGTT	GCCGTGGCTTACATCAAAGT	(14)
Hbb†	TGCATGTGGATCCTGAGAAC	GTGAAATCCTTGCCCAGGT	(14)
Id1	AACGGCGAGATCAGTGCCTT	GAGTCCATCTGGTCCCTCAGTG	(15)
Tmprss6	CGCTGGGTCATAACGGC	AACAGACGGCTCACCTTG	This study

*This primer set recognizes mRNAs transcribed from both the murine *Hba-a1* and *Hba-a2* loci.

†This primer set recognizes mRNAs transcribed from both the murine *Hbb-b1* and *Hbb-b2* loci.

Legends to Supplementary Figures

Supplementary Figure 1. Genetic loss of *Tmprss6* modifies tissue iron loading and splenomegaly in female *Hbb*$^{th3/+}$ mice. Tissue non-heme iron concentration (NHIC) and spleen weight were analyzed in 8-week-old female mice of different *Hbb-Tmprss6* genotypes. Graphed are mean values obtained from analyses of NHIC of liver (A), spleen (B), kidney (C), heart (D), and pancreas (E), and analysis of spleen weight (F). Error bars represent SD. **P*<.001 compared with *Hbb*$^{+/+}$*Tmprss6*$^{+/+}$; †*P*<.001 compared with *Hbb*$^{th3/+}$*Tmprss6*$^{+/+}$; ‡*P* value not significant compared with *Hbb*$^{+/+}$*Tmprss6*$^{-/-}$; §*P*<.05 compared with *Hbb*$^{+/+}$*Tmprss6*$^{+/+}$; and ||*P*<.05 compared with *Hbb*$^{th3/+}$*Tmprss6*$^{+/+}$ mice. For each parameter shown, the number of mice per genotype analyzed was as follows (exceptions shown in parentheses): 7 *Hbb*$^{+/+}$*Tmprss6*$^{+/+}$, 8 *Hbb*$^{+/+}$*Tmprss6*$^{+/-}$ (7 for pancreas), 9 *Hbb*$^{+/+}$*Tmprss6*$^{-/-}$ (8 for kidney), 7 *Hbb*$^{th3/+}$*Tmprss6*$^{+/+}$ (6 for spleen weight), 9 *Hbb*$^{th3/+}$*Tmprss6*$^{+/-}$, and 8 *Hbb*$^{th3/+}$*Tmprss6*$^{-/-}$. Mice were fed a 270 p.p.m. iron diet.

Supplementary Figure 2. Genetic loss of *Tmprss6* modifies tissue iron loading and splenomegaly in male *Hbb*$^{th3/+}$ mice. Tissue NHIC and spleen weight were analyzed in 8-week-old male mice of different *Hbb-Tmprss6* genotypes. Graphed are mean values obtained from analyses of NHIC of liver (A), spleen (B), kidney (C), heart (D), and pancreas (E), and analysis of spleen weight (F). Error bars represent SD. **P*<.001 compared with *Hbb*$^{+/+}$*Tmprss6*$^{+/+}$; †*P*<.05 compared with *Hbb*$^{th3/+}$*Tmprss6*$^{+/+}$; ‡*P*<.001 compared with *Hbb*$^{th3/+}$*Tmprss6*$^{+/+}$; §*P* value not significant compared with *Hbb*$^{+/+}$*Tmprss6*$^{-/-}$; and ||*P*<.05 compared with *Hbb*$^{+/+}$*Tmprss6*$^{+/+}$ mice. For each parameter shown, the number of mice per genotype analyzed was as follows (exception shown in parentheses): 7 *Hbb*$^{+/+}$*Tmprss6*$^{+/+}$, 8 *Hbb*$^{+/+}$*Tmprss6*$^{+/-}$, 8 *Hbb*$^{+/+}$*Tmprss6*$^{-/-}$, 8

Hbb$^{th3/+}$*Tmprss6*$^{+/+}$, 8 *Hbb*$^{th3/+}$*Tmprss6*$^{+/-}$ (7 for spleen iron), and 8 *Hbb*$^{th3/+}$*Tmprss6*$^{-/-}$. Mice were fed a 270 p.p.m. iron diet.

Supplementary Figure 3. Genetic loss of *Tmprss6* alters expression of genes related to the Bmp/Smad signaling pathway in livers of female *Hbb*$^{th3/+}$ mice. Graphed is the mean hepatic mRNA expression of *Bmp6* (A), *Bmp2* (B), *Hamp* (C), *Id1* (D), *Atoh8* (E), and *Tmprss6* (F) relative to β-actin (*Actb*) in 8-week-old female mice of selected *Hbb-Tmprss6* genotypes. Because we previously found that heterozygous *Tmprss6* disruption does not significantly alter *Hamp* or *Id1* expression in wild-type mice at this age,(1) *Hbb*$^{+/+}$*Tmprss6*$^{+/-}$ mice were not analyzed so that a larger number of samples from the other genotypes could be analyzed in parallel on the same quantitative PCR plate. Ratios of mRNA expression are normalized to an *Hbb*$^{+/+}$*Tmprss6*$^{+/+}$ mean value of 1. Error bars represent SD. For each panel, 6 *Hbb*$^{+/+}$*Tmprss6*$^{+/+}$, 9 *Hbb*$^{+/+}$*Tmprss6*$^{-/-}$, 7 *Hbb*$^{th3/+}$*Tmprss6*$^{+/+}$, 9 *Hbb*$^{th3/+}$*Tmprss6*$^{+/-}$, and 7 *Hbb*$^{th3/+}$*Tmprss6*$^{-/-}$ mice were analyzed. *NS*, not significant. Mice were fed a 270 p.p.m. iron diet.

Supplementary Figure 4. Genetic loss of *Tmprss6* alters expression of genes related to the Bmp/Smad signaling pathway in livers of male *Hbb*$^{th3/+}$ mice. Graphed is the mean hepatic mRNA expression of *Bmp6* (A), *Hamp* (B), *Id1* (C), *Atoh8* (D), and *Tmprss6* (E) relative to β-actin (*Actb*) in 8-week-old male mice of selected *Tmprss6-Hbb* genotypes. *Hbb*$^{+/+}$*Tmprss6*$^{+/-}$ mice were not analyzed so that a larger number of samples from the other genotypes could be analyzed in parallel on the same quantitative PCR plate. To enable comparisons with the expression levels measured in female mice, mRNA expression ratios were normalized such that a ratio of 1 corresponds to the mean mRNA expression ratio observed in female *Hbb*$^{+/+}$*Tmprss6*$^{+/+}$ mice in *Supplementary Figure 3*. Error bars represent SD. For each panel, 7 *Hbb*$^{+/+}$*Tmprss6*$^{+/+}$, 9

Hbb$^{+/+}$*Tmprss6*$^{-/-}$, 8 *Hbb*$^{th3/+}$*Tmprss6*$^{+/+}$, 8 *Hbb*$^{th3/+}$*Tmprss6*$^{+/-}$, and 9 *Hbb*$^{th3/+}$*Tmprss6*$^{-/-}$ mice were analyzed. Mice were fed a 270 p.p.m. iron diet.

Supplementary Figure 5. Genetic loss of *Tmprss6* in *Hbb*$^{th3/+}$ mice alters erythrocyte morphology and reduces extramedullary hematopoiesis in spleen. Shown are modified Wright-Giemsa stained peripheral blood smears (A) and hematoxylin and eosin stained histological sections of spleen (B) from 8-week-old female mice of selected *Hbb-Tmprss6* genotypes. Representative results from examination of 3 mice per genotype (females, 8-weeks-old) are shown. Original magnification x1000 (A) and x40 (B). Mice were fed a 270 p.p.m. iron diet.

Supplementary Figure 6. Globin chain mRNA ratios remain imbalanced in *Hbb* mice with genetic loss of *Tmprss6*. Graphed for male mice (8-9 weeks old) of selected *Hbb-Tmprss6* genotypes is the mean ratio of mRNA encoding β-globin (*Hbb*) relative to α-globin (*Hba*) in total BM (A) and spleen (B). mRNA expression ratios are normalized to an *Hbb*$^{+/+}$*Tmprss6*$^{+/+}$ mean value of 1. Error bars represent SD. **P*<.005 compared with *Hbb*$^{+/+}$*Tmprss6*$^{+/+}$ and †*P*<.005 compared with *Hbb*$^{th3/+}$*Tmprss6*$^{+/+}$. The number of mice analyzed was as follows, with exception shown in parenthesis: 7 *Hbb*$^{+/+}$*Tmprss6*$^{+/+}$, 7 *Hbb*$^{+/+}$*Tmprss6*$^{-/-}$, 5 *Hbb*$^{th3/+}$*Tmprss6*$^{+/+}$, and 7 *Hbb*$^{th3/+}$*Tmprss6*$^{-/-}$ (8 in panel B). Mice were fed a 200 p.p.m. iron diet.

Supplementary Figure 7. Genetic loss of *Tmprss6* alters the erythropoietic composition of spleen of *Hbb*$^{th3/+}$ mice. Erythroid (TER-119^{+}) cells from spleen of mice of selected *Hbb-Tmprss6* genotypes were grouped by stage of erythroid maturation based on forward scatter and CD44 expression, as illustrated in *Supplementary Figure 9*. (A) Graphed is the mean percentage of total splenic cells composed of TER-119^{+} cells distributed in regions I, II, III, IV, and V, respectively. (B) Graphed on a log scale is the mean fluorescence intensity of CD71 expression in splenic EP

distributed in regions I-III. (C) Graphed is the mean percentage of apoptotic (annexin V^+) splenic erythroid cells distributed in regions IV and V. Graphed is the mean fluorescence intensity of splenic erythroid cells distributed in region IV (D) and in region V (E) generated following incubation with the ROS indicator CM-H_2DCFDA. Error bars represent SD. For all panels, tissues from female mice (8-11 weeks old) were analyzed. *P<.005 compared with *Hbb*$^{+/+}$*Tmprss6*$^{+/+}$; † P value not significant compared with *Hbb*$^{+/+}$*Tmprss6*$^{-/-}$; ‡P<.05 compared with *Hbb*$^{+/+}$*Tmprss6*$^{+/+}$; §P<.005 compared with *Hbb*$^{th3/+}$*Tmprss6*$^{+/+}$; ||P<.05 compared with *Hbb*$^{th3/+}$*Tmprss6*$^{+/+}$; For panel A, the number of mice per genotype analyzed was 5 *Hbb*$^{+/+}$*Tmprss6*$^{+/+}$, 5 *Hbb*$^{+/+}$*Tmprss6*$^{-/-}$, 4 *Hbb*$^{th3/+}$*Tmprss6*$^{+/+}$, and 6 *Hbb*$^{th3/+}$*Tmprss6*$^{-/-}$. For panel B, the number of mice analyzed was 4 *Hbb*$^{+/+}$*Tmprss6*$^{+/+}$, 4 *Hbb*$^{+/+}$*Tmprss6*$^{-/-}$, 3 *Hbb*$^{th3/+}$*Tmprss6*$^{+/+}$, and 5 *Hbb*$^{th3/+}$*Tmprss6*$^{-/-}$. For panel C, the number of mice per genotype analyzed was 5 *Hbb*$^{+/+}$*Tmprss6*$^{+/+}$, 5 *Hbb*$^{+/+}$*Tmprss6*$^{-/-}$, 4 *Hbb*$^{th3/+}$*Tmprss6*$^{+/+}$, and 5 *Hbb*$^{th3/+}$*Tmprss6*$^{-/-}$. For panels D and E, the number of mice per genotype analyzed was 4 *Hbb*$^{+/+}$*Tmprss6*$^{+/+}$, 4 *Hbb*$^{+/+}$*Tmprss6*$^{-/-}$, 3 *Hbb*$^{th3/+}$*Tmprss6*$^{+/+}$, and 4 *Hbb*$^{th3/+}$*Tmprss6*$^{-/-}$. Mice were fed a 200 p.p.m. iron diet.

Supplementary Figure 8. Genetic loss of *Tmprss6* lowers hepatic *Epo* mRNA levels in *Hbb*$^{th3/+}$ mice. Graphed is the mean hepatic *Epo* mRNA expression relative to β-actin (*Actb*) in 8-week-old female mice of selected *Hbb-Tmprss6* genotypes. To enable a comparison with the kidney *Epo* mRNA expression shown in *Figure 3*, the hepatic *Epo*-to-*Actb* mRNA ratios are normalized so that a mRNA ratio of 1 corresponds to the mean *Epo*-to-*Actb* mRNA ratio measured in *Hbb*$^{+/+}$*Tmprss6*$^{+/+}$ kidney (from *Figure 3A*). Error bars represent SD. Animal group sizes were identical to those in *Supplementary Figure 3*. Mice were fed a 270 p.p.m. iron diet.

Supplementary Figure 9. Illustration of the flow cytometry analysis methods used to assess CD71 expression, ROS activity, and apoptosis in erythroid populations. Erythroid-

committed (TER-119$^+$) bone marrow cells were analyzed to discern stages of erythroid maturation as shown in Panel A, and erythroid cells within each maturation stage were then further analyzed for CD71 expression, ROS activity, and apoptosis as shown in Panels B, C, and D, respectively. Representative flow cytometry plots are presented for 1 *Hbb*$^{+/+}$*Tmprss6*$^{+/+}$, 1 *Hbb*$^{th3/+}$*Tmprss6*$^{+/+}$, and 1 *Hbb*$^{th3/+}$*Tmprss6*$^{-/-}$ mouse. (A) Assessment of maturation of TER-119$^+$ bone marrow cells based on forward light scatter (FSC, an indicator of cell size) and CD44 expression. The decreases in cell size and CD44 expression that occur during erythroid maturation enable TER-119$^+$ cells to be grouped into regions I (least mature) through V (most mature), using contour plots (not shown) to position the boundaries between regions.(5) Plots are presented in pseudocolor to highlight the differences in cell density in maturing erythroid populations observed in different genotypes. Numbers indicate the percentage of TER-119$^+$ cells located within each gate. Note that in the *Hbb*$^{th3/+}$*Tmprss6*$^{-/-}$ mouse, cells in regions IV and V show lower forward scatter, consistent with the extreme microcytosis observed in peripheral red blood cells from this genotype. (B) Assessment of CD71 expression within different erythroid populations defined by FSC and CD44 expression. Shown are representative histograms plotting the fluorescence intensity of CD71 expression detected for TER-119$^+$ bone marrow cells within region II. Statistical comparisons were calculated from the geometric mean of CD71 fluorescence intensity detected across the population. (C) Assessment of ROS activity within different erythroid populations defined by FSC and CD44 expression. Shown are representative histograms plotting the fluorescence intensity generated following incubation with the ROS indicator CM-H_2DCFDA detected for TER-119$^+$ bone marrow cells within region IV. Statistical comparisons were calculated from the geometric mean of ROS fluorescence intensity detected across the population. (D) Assessment of apoptosis within different erythroid populations defined by FSC and CD44 expression. Shown are representative histograms plotting the fluorescence intensity resulting from binding of the apoptosis indicator annexin V detected for TER-119$^+$ bone marrow cells within region IV. Cells with fluorescence greater than the specified threshold (bracket) were defined as

annexin V+. The same fluorescence threshold was applied across all samples. Statistical comparisons were based on the percentage of annexin V positive cells in each sample. In spleen, cells were analyzed using the same approaches demonstrated in panels A-D, defining erythroid commitment based on TER-119 positivity. However, to improve accuracy of erythroid subpopulation classification, events with extremely bright TER-119-staining, which possessed non-erythroid light scatter properties, were excluded from analysis. For the assessments illustrated in panels A-D, results from *Hbb*$^{+/+}$*Tmprss6*$^{-/-}$ mice were extremely similar to *Hbb*$^{th3/+}$*Tmprss6*$^{-/-}$ mice.

Supplementary Figure 1

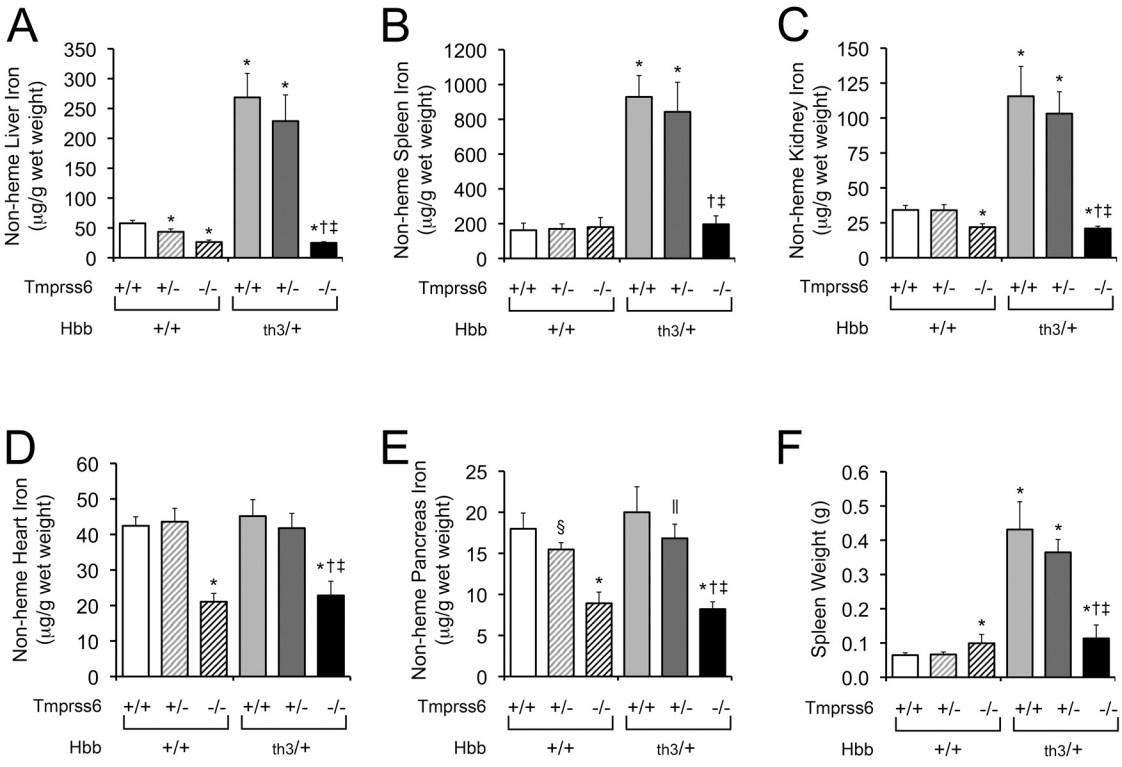

Supplementary Figure 2

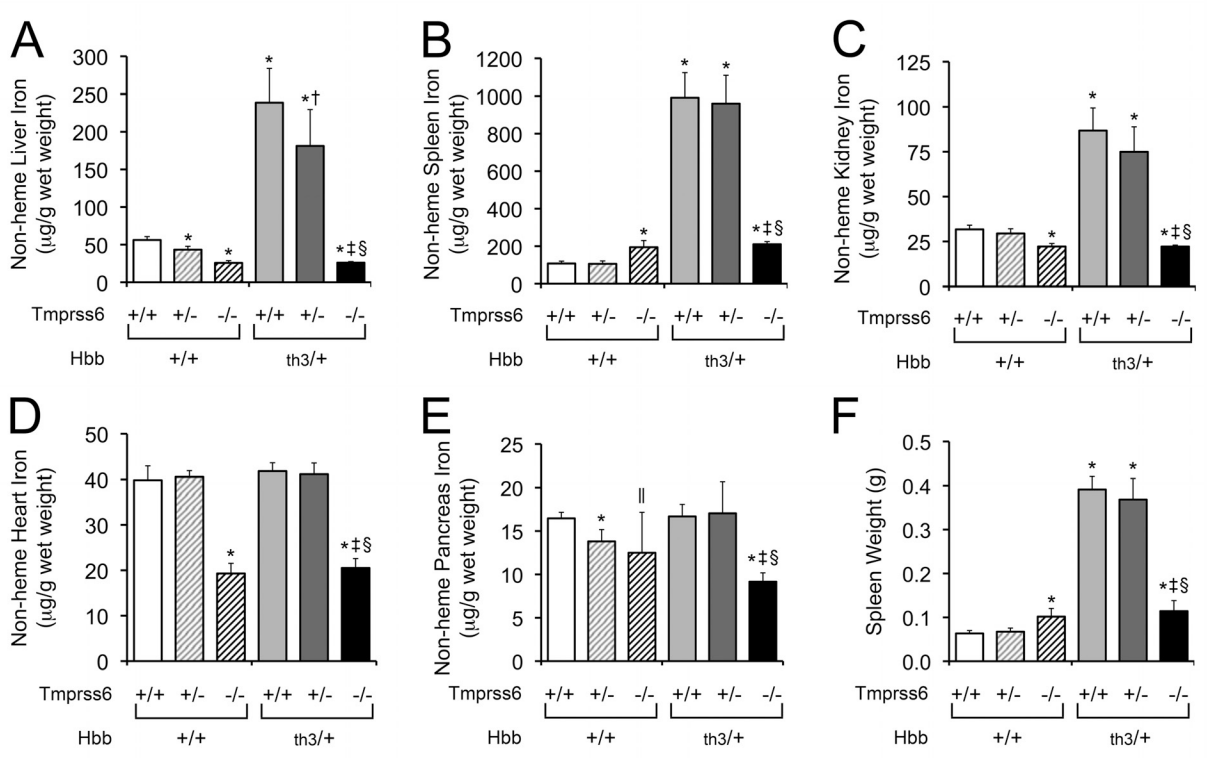

Supplementary Figure 3

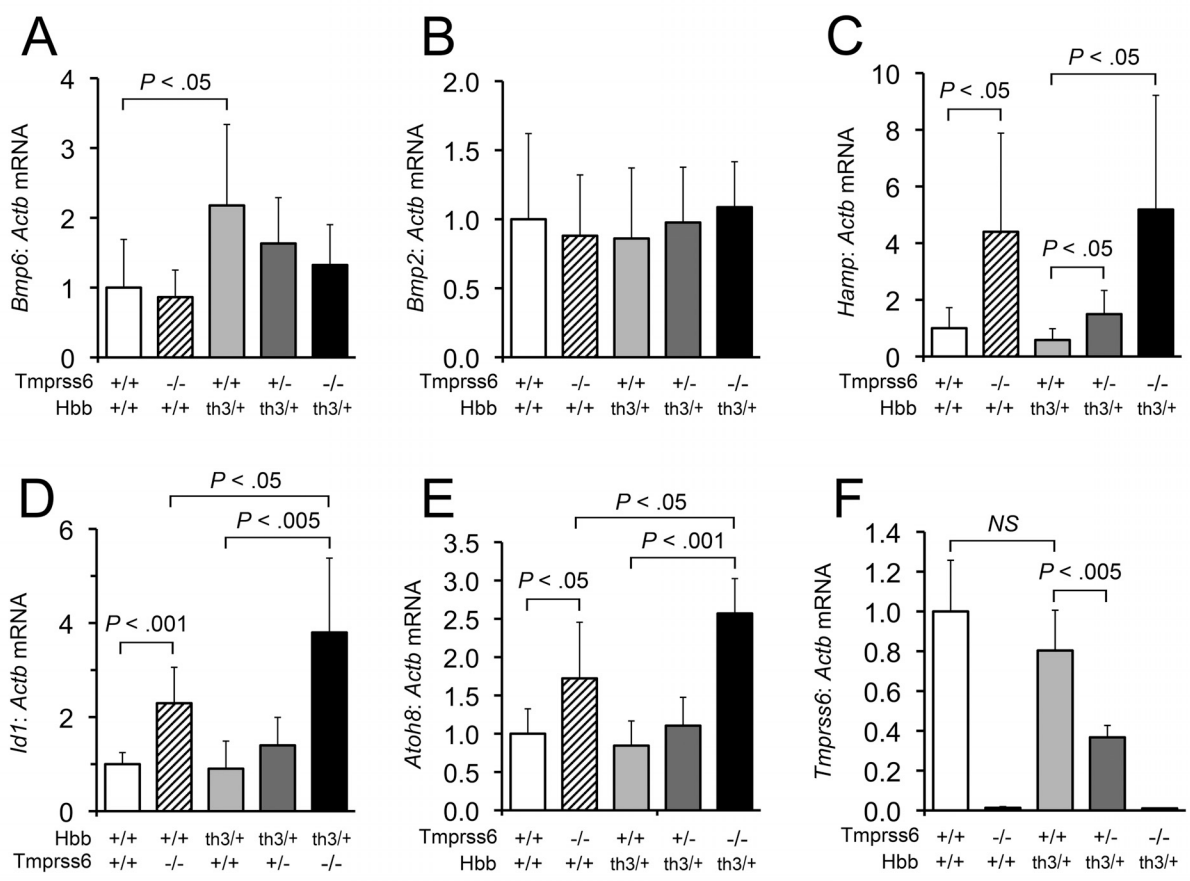

Supplementary Figure 4

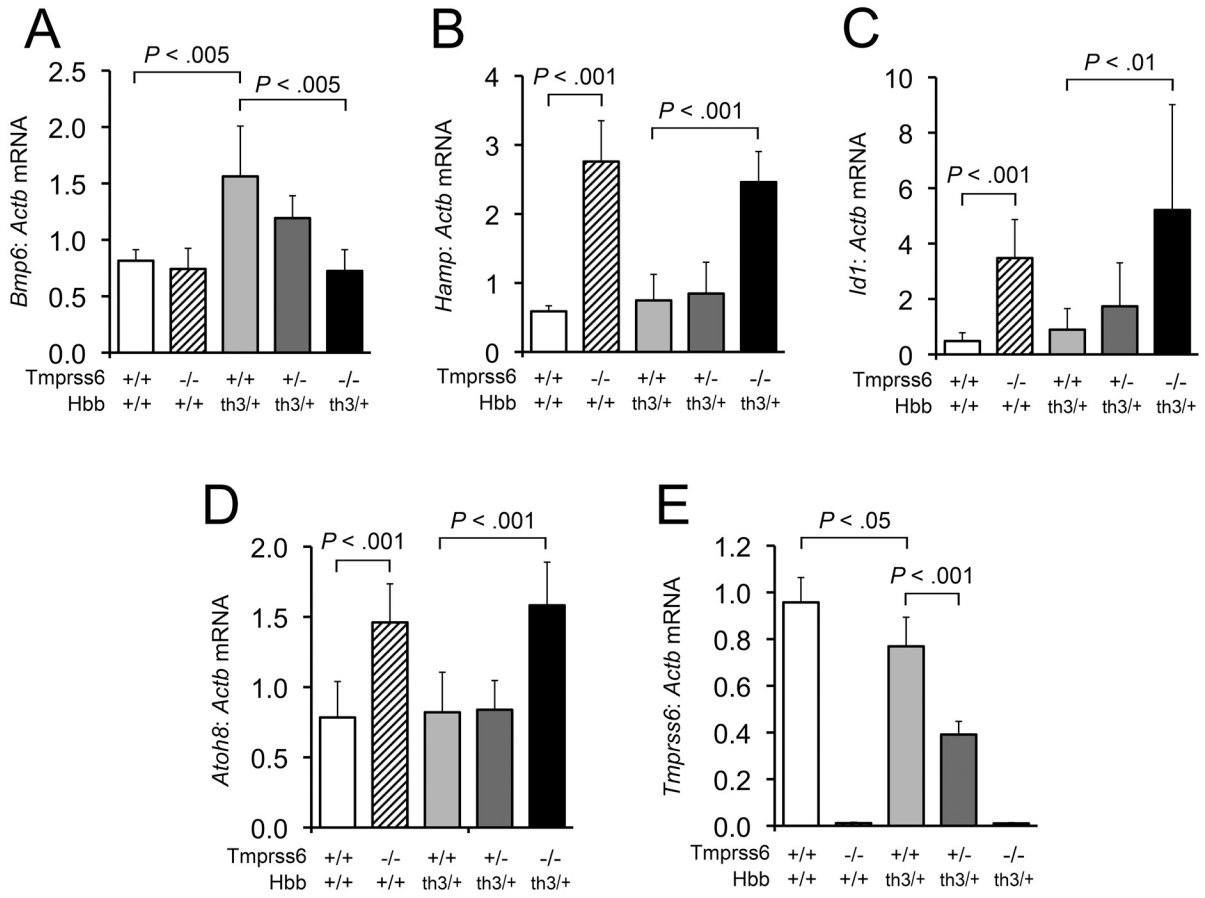

Supplementary Figure 5

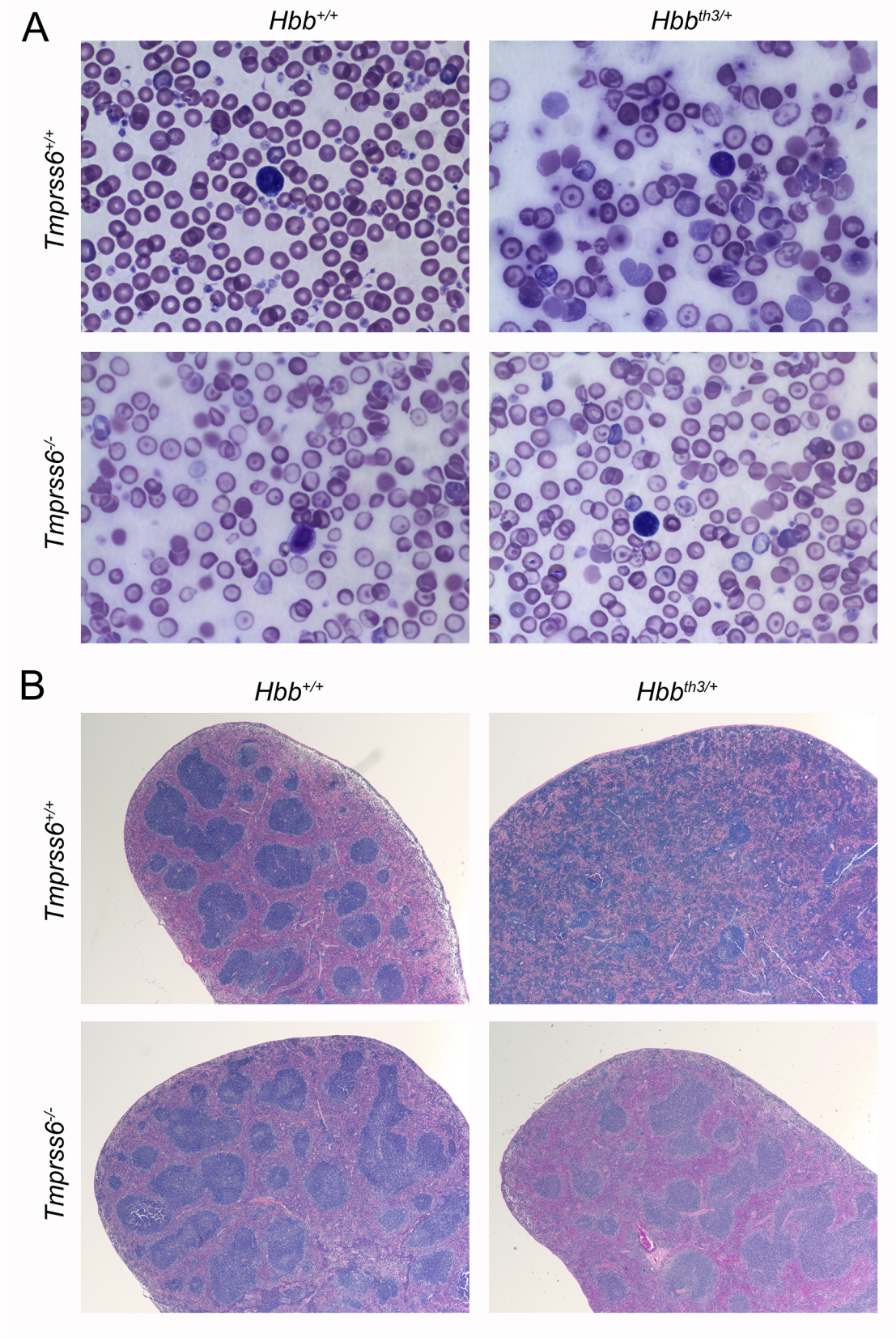

Supplementary Figure 6

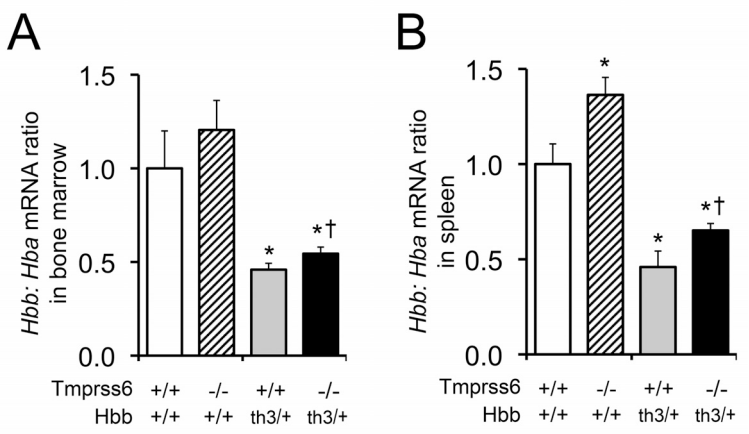

Supplementary Figure 7

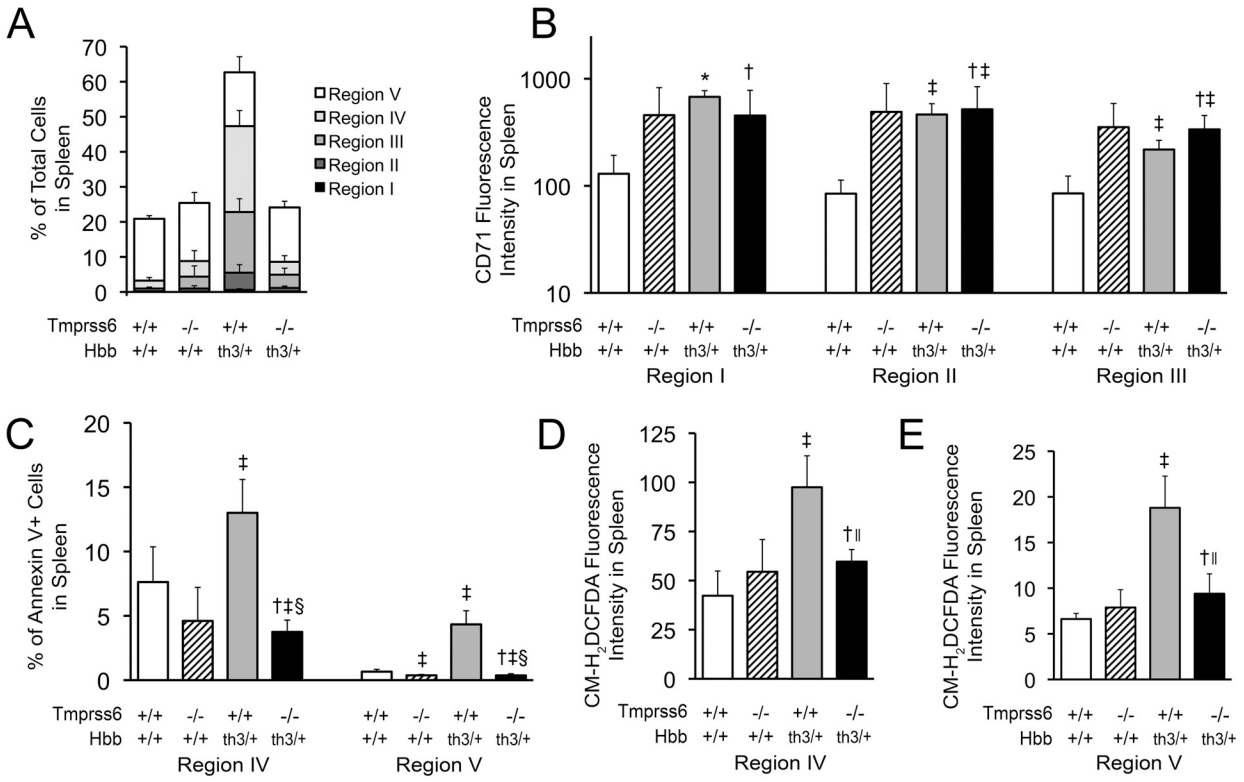

Supplementary Figure 8

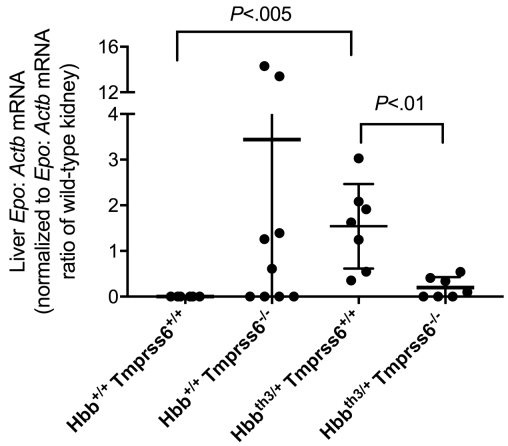

Supplementary Figure 9

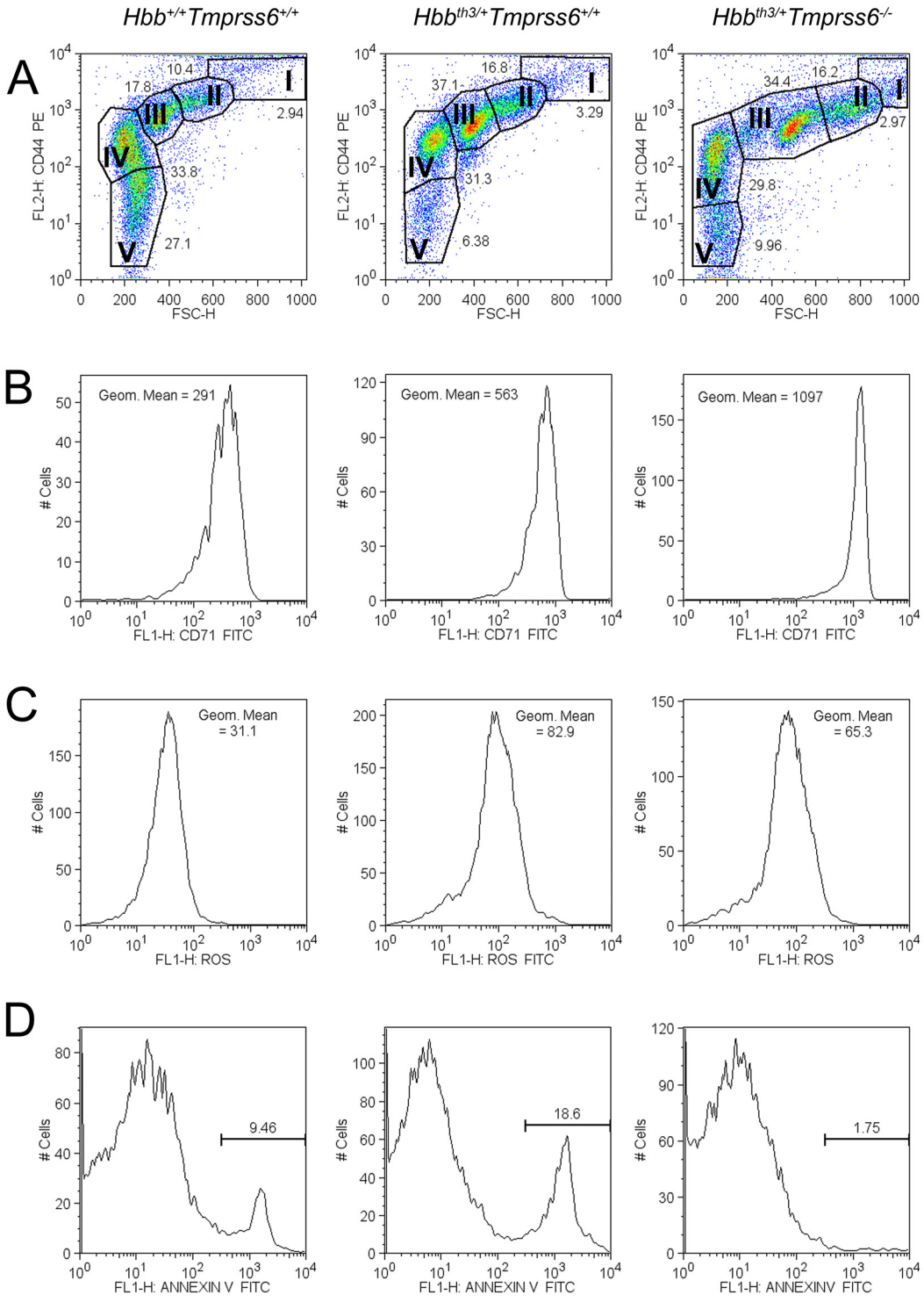

Supplementary References

1. Finberg KE, Whittlesey RL, Fleming MD, Andrews NC. Down-regulation of Bmp/Smad signaling by Tmprss6 is required for maintenance of systemic iron homeostasis. Blood. 2010;115(18):3817-26.
2. Yang B, Kirby S, Lewis J, Detloff PJ, Maeda N, Smithies O. A mouse model for beta 0-thalassemia. Proc Natl Acad Sci U S A. 1995;92(25):11608-12.
3. Torrance JD, Bothwell TH. Tissue Iron Stores. In: Cook JD, ed. Methods in Hematology: Iron. New York: Churchill Livingstone, 1980:90-115.
4. Kong Y, Zhou S, Kihm AJ, et al. Loss of alpha-hemoglobin-stabilizing protein impairs erythropoiesis and exacerbates beta-thalassemia. J Clin Invest. 2004;114(10):1457-66.
5. Chen K, Liu J, Heck S, Chasis JA, An X, Mohandas N. Resolving the distinct stages in erythroid differentiation based on dynamic changes in membrane protein expression during erythropoiesis. Proc Natl Acad Sci U S A. 2009;106(41):17413-8.
6. Gardenghi S, Ramos P, Marongiu MF, et al. Hepcidin as a therapeutic tool to limit iron overload and improve anemia in beta-thalassemic mice. J Clin Invest. 2010;120(12):4466-77.
7. Schmidt PJ, Toran PT, Giannetti AM, Bjorkman PJ, Andrews NC. The transferrin receptor modulates Hfe-dependent regulation of hepcidin expression. Cell Metab. 2008;7(3):205-14.
8. Wang B, Fang Y, Guo X, Ren Z, Zhang J. Transgenic human alpha-hemoglobin stabilizing protein could partially relieve betaIVS-2-654-thalassemia syndrome in model mice. Hum Gene Ther. 2010;21(2):149-56.
9. Kautz L, Meynard D, Monnier A, et al. Iron regulates phosphorylation of Smad1/5/8 and gene expression of Bmp6, Smad7, Id1, and Atoh8 in the mouse liver. Blood. 2008;112(4):1503-9.
10. Chen H, Choesang T, Li H, et al. Increased hepcidin in transferrin-treated thalassemic mice correlates with increased liver BMP2 expression and decreased hepatocyte ERK activation. Haematologica. 2016;101(3):297-308.
11. Kautz L, Jung G, Valore EV, Rivella S, Nemeth E, Ganz T. Identification of erythroferrone as an erythroid regulator of iron metabolism. Nat Genet. 2014;46(7):678-84.
12. Kim KS, Zhang DL, Kovtunovych G, et al. Infused wild-type macrophages reside and self-renew in the liver to rescue the hemolysis and anemia of Hmox1-deficient mice. Blood Adv. 2018;2(20):2732-43.
13. Bartnikas TB, Andrews NC, Fleming MD. Transferrin is a major determinant of hepcidin expression in hypotransferrinemic mice. Blood. 2011;117(2):630-7.
14. Choi YG, Yeo S, Hong YM, Kim SH, Lim S. Changes of gene expression profiles in the cervical spinal cord by acupuncture in an MPTP-intoxicated mouse model: microarray analysis. Gene. 2011;481(1):7-16.
15. Andriopoulos B, Jr., Corradini E, Xia Y, et al. BMP6 is a key endogenous regulator of hepcidin expression and iron metabolism. Nat Genet. 2009;41(4):482-7.